

Excitation functions of $^{nat}\text{Pb}(\text{d},\text{x})^{206,205,204,203,202}\text{Bi}$, $^{203\text{cum},202\text{m},201\text{cum}}\text{Pb}$ and $^{202\text{cum},201\text{cum}}\text{Tl}$ reactions up to 50 MeV

F. Ditrói · F. Tárkányi · S. Takács · A. Hermanne · A.V. Ignatyuk

Received: 2014 / Accepted: 2014

Abstract Cross-sections of deuteron induced nuclear reactions on lead were measured up to 50 MeV using the standard stacked foil irradiation technique and high resolution γ -ray spectrometry. Experimental cross-sections and derived integral yields are presented for the $^{nat}\text{Pb}(\text{d},\text{x})^{206,205,204,203,202}\text{Bi}$, $^{203\text{cum},202\text{m},201\text{cum}}\text{Pb}$ and $^{202\text{cum},201\text{cum}}\text{Tl}$ reactions. The experimental data were compared with the results from literature and with the data in the TENDL-2013 library (obtained with TALYS code). The cross-section data were analyzed also with the theoretical results calculated by using the ALICE-IPPPE-D and EMPIRE-D codes.

Keywords: lead target; deuteron irradiation; Bi, Pb and Tl radioisotopes; integral yield

1 Introduction

In the frame of our systematic study of activation cross-sections of deuteron induced nuclear reactions for different applications and for development of the reaction models [1,2] we have investigated the activation cross-sections on lead. In an earlier study we have already presented the excitation functions for longer lived activa-

tion products up to 40 MeV [3] ($^{nat}\text{Pb}(\text{d},\text{xn})^{203,204,205,206,207}\text{Bi}$, $^{nat}\text{Pb}(\text{d},\text{x})^{203}\text{Pb}$, ^{202}Tl reactions). In this work we have extended the energy range up to 50 MeV and we have tried to obtain data also for shorter-lived products. A literature search resulted in only one additional cross-section study reported by Wasilyeski et al. [4] up to 27 MeV while experimental integral yield data in the 11-22 MeV energy range were measured by Dmitriev et al. [5].

2 Experimental

The experimental techniques and data analysis were similar or identical as described by us in recent publications (c.f. [6,7,8,9]). Here we present shortly the most important facts, and details specific for this experiment. Taking into account the large energy range to be covered the foil stacks were irradiated at two incident energies (50 MeV and 21 MeV). The first stack (series 1), containing ^{nat}Eu (100 μm), Sb(2 μm) evaporated onto Kapton foil (13 μm), Pb (15.74 μm) and Tb (95.47 μm) target foils interleaved with 49.06 μm Al monitor foils was irradiated at the Cyclone 90 cyclotron of the Universit Catholique in Louvain la Neuve (LLN) with a 50 MeV incident energy deuteron beam (60 min, 150 nA). A second stack (series 2) containing ^{nat}Pb (15.74 μm) target foils, Al energy degrader/monitor foils (50 μm), was irradiated at the CGR 560 cyclotron of the Vrije Universiteit Brussel (VUB) with a 21 MeV incident energy deuteron beam (60 min, 105 nA). The activity produced in the targets and monitor foils was measured non-destructively (without chemical separation) using a high resolution HPGe γ -ray spectrometer. For the high energy irradiation four series of measurements were performed starting at about 4 h, 50 h, 450 h and

F. Ditrói · F. Tárkányi · S. Takács
Institute for Nuclear Research, Hungarian Academy of Sciences
Tel.: +36-52-509251
Fax: +36-52-416181
E-mail: ditroi@atomki.hu

A. Hermanne
Cyclotron Laboratory, Vrije Universiteit Brussel (VUB),
Brussels, Belgium

A.V. Ignatyuk
Institute of Physics and Power Engineering (IPPE), Obninsk
249020, Russia

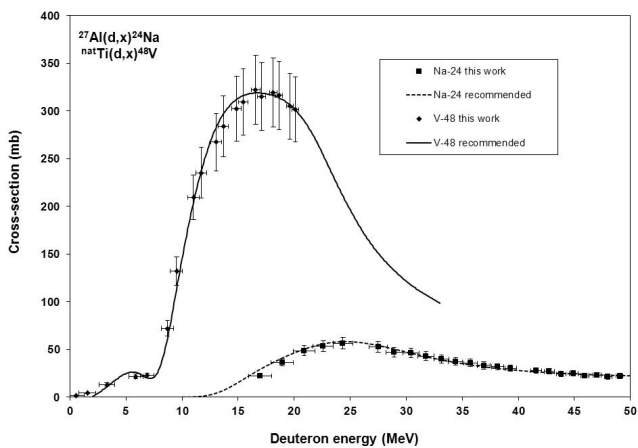


Fig. 1 The re-measured cross-sections of the used monitor reactions in comparison with the recommended data.

2200 h after EOB at 50, 25 and 5 cm source-detector distances. Also four series of γ -spectra measurements were done for the low energy experiment starting at about 1 h, 4 h, 45 h and 770 h after EOB and at 20, 15 and 5 cm source-detector distances. The decay data of the investigated activation products, taken from the on-line database NuDat2 [10] are summarized in Table 1 together with the possibly contributing reactions and their thresholds. Effective incident beam energy and the energy scale were determined primary by calculation [11] and finally by using the excitation functions of the $^{24}\text{Al}(d,x)^{24}\text{Na}$ and $^{nat}\text{Ti}(d,x)^{48}\text{V}$ monitor reactions [12] simultaneously re-measured over the whole energy range. The beam intensity (the number of the incident particles) was initially obtained through measuring the charge collected in a short Faraday cup and, if needed, adapted on the basis of the monitor reactions. The curve of the re-measured excitation function in comparison with the IAEA recommended data [8] can be found in Fig. 1. The uncertainty of the median energy in each foil was estimated taking into account the cumulative effects of possible uncertainties (primary energy, target thickness, energy straggling, correction to monitor reaction). The uncertainty of the cross-sections was obtained as the sum in quadrature of all linear contributions of systematic uncertainties (beam current (7%), beam-loss corrections (max. of 1.5%), target thickness (1%), detector efficiency (5%), γ -intensities (3%) and the individual uncertainty of the photo peak area determination (counting statistics :1-20%).

Table 1 Decay characteristic of the investigated reaction products

Nuclide	Half-life	E_γ (keV)	I_γ (%)	Contributing reaction	Q-value (keV)
^{207}Bi ϵ : 100 %	31.55 a	569.698	97.75	$^{206}\text{Pb}(d,n)$	1333.45
		1063.656	74.5	$^{207}\text{Pb}(d,2n)$	-5404.32
				$^{208}\text{Pb}(d,3n)$	12772.19
^{206}Bi ϵ : 100 %	6.243 d	183.977	15.8	$^{206}\text{Pb}(d,2n)$	-6764.22
		343.51	23.5	$^{207}\text{Pb}(d,3n)$	-13502.0
		398.00	10.75	$^{208}\text{Pb}(d,4n)$	-20869.86
		497.06	15.33		
		516.18	40.8		
		537.45	30.5		
		803.10	99.0		
881.01	66.2				
895.12	15.67				
1098.26	13.51				
^{205}Bi ϵ : 100 %	15.31 d	703.45	31.1	$^{204}\text{Pb}(d,n)$	1019.19
		987.66	16.1	$^{206}\text{Pb}(d,3n)$	-13799.13
		1764.30	32.5	$^{207}\text{Pb}(d,4n)$	-20536.91
				$^{208}\text{Pb}(d,5n)$	-27904.78
^{204}Bi ϵ : 99.75% β^+ : 0.25 %	11.22 h	374.76	82	$^{204}\text{Pb}(d,2n)$	-7470.71
		670.72	11.4	$^{206}\text{Pb}(d,4n)$	-22289.04
		899.15	99	$^{207}\text{Pb}(d,5n)$	-29026.81
		911.74	13.6	$^{208}\text{Pb}(d,6n)$	-36394.68
		911.96	11.2		
		918.26	10.9		
		983.98	59		
^{203}Bi ϵ : 100 %	11.76 h	816.3	4.1	$^{204}\text{Pb}(d,3n)$	-14663.4
		820.2	30.0	$^{206}\text{Pb}(d,5n)$	-29481.7
		825.2	14.8	$^{207}\text{Pb}(d,6n)$	-36219.5
		847.2	8.6	$^{208}\text{Pb}(d,7n)$	-43587.3
		896.9	13.2		
		1033.7	8.9		
1679.6	8.9				
^{202}Bi ϵ : 100 %	1.71 h	422.13	83.7	$^{204}\text{Pb}(d,4n)$	-23518.1
		657.49	60.6	$^{206}\text{Pb}(d,6n)$	-38336.5
		960.67	99.283	$^{207}\text{Pb}(d,7n)$	-45074.2
				$^{208}\text{Pb}(d,8n)$	-52442.1
^{203}Pb ϵ : 100 %	51.92 h	279.1952	80.9	$^{204}\text{Pb}(d,p2n)$	-10619.24
				$^{206}\text{Pb}(d,p4n)$	-25437.57
				$^{207}\text{Pb}(d,p5n)$	-32175.35
				$^{208}\text{Pb}(d,p6n)$	-39543.22
				^{203}Bi decay	
^{202m}Pb ϵ : 9.5 % IT: 90.5 % 2169.83 keV	3.54 h	422.12	84	$^{204}\text{Pb}(d,p3n)$	-
		657.49	31.7	$^{206}\text{Pb}(d,p5n)$	17536.35
		786.99	49	$^{207}\text{Pb}(d,p6n)$	-32354.67
		960.70	89.9	$^{208}\text{Pb}(d,p7n)$	-39092.45
^{201}Pb $\epsilon \leq 100$ % β^+ : 0.064 %	9.33 h	331.15	77	$^{204}\text{Pb}(d,p4n)$	-26288.5
		907.67	6.7	$^{206}\text{Pb}(d,p6n)$	-41106.8
		945.96	7.2	$^{207}\text{Pb}(d,p7n)$	-47844.6
				$^{208}\text{Pb}(d,p8n)$	-55212.5
				^{201}Bi decay	
^{202}Tl ϵ : 100 %	12.31 d	39.510	91.5	$^{204}\text{Pb}(d,2p2n)$	-16707.8
				$^{206}\text{Pb}(d,2p4n)$	-31526.1
				$^{207}\text{Pb}(d,2p5n)$	-38263.9
				$^{208}\text{Pb}(d,2p6n)$	-45631.8
				^{202}Pb decay	
^{201}Tl ϵ : 100 %	3.0421 d	135.34	2.565	$^{204}\text{Pb}(d,2p3n)$	-23586.6
		167.43	10.0	$^{206}\text{Pb}(d,2p5n)$	-38404.9
				$^{207}\text{Pb}(d,2p6n)$	-45142.7
				$^{208}\text{Pb}(d,2p7n)$	-52510.6
				^{201}Pb decay	

When complex particles are emitted instead of individual protons and neutrons the Q-values have to be modified by the respective binding energies of the compound particles: np-d, +2.2 MeV; 2np-t, +8.48 MeV; 2p2n-a, 28.30 MeV.
*Decrease Q-values for isomeric states with level energy of the isomer

3 Results and discussion

3.1 Theoretical calculations

For theoretical estimation the updated ALICE-IPPE-D [13] and EMPIRE-D [14] codes were used. In the modified versions of the codes [15,16] a simulation of direct (d,p) and (d,t) transitions by the general relations for a nucleon transfer probability in the continuum is included through an energy dependent enhancement

factor for the corresponding transitions based on systematic of experimental data [17]. Results of ALICE-IPPE-D for excited states were obtained by applying the isomeric ratios derived from the EMPIRE-D code to the total cross-sections calculated by ALICE-IPPE-D. For a comparison with the experiments the theoretical data from the successive TENDL-2009-2010-2011-2012 and TENDL-2013 libraries [18] (based on the modified TALYS code [19]) were used too to see the evolution of prediction capability and performance of the new versions.

3.2 Excitation functions

The cross-sections for radionuclides produced in the bombardment of ^{nat}Pb with deuterons are tabulated in Tables 2 and 3 respectively, and are shown graphically in Figs 2-13 for comparison with the theory and with the earlier experimental results. By irradiating lead with natural isotopic abundance (^{204}Pb -1.4 %, ^{206}Pb -24.1 %, ^{207}Pb -22.1 % and ^{208}Pb -52.4 %) with 50 MeV deuterons, radioisotopes of Bi, Pb and Tl are produced in significant amounts. We did not obtain reliable data for production of a few Bi, Pb and Tl radionuclides. Among the radio-products formed ^{208}Bi ($T_{1/2} = 3.68 \cdot 10^{55}$ a) and ^{205}Pb ($T_{1/2} = 1.73 \cdot 10^7$ a), ^{202g}Pb ($T_{1/2} = 5.25 \cdot 10^3$ a) have too long half-lives. The nuclides ^{209}Pb and ^{204}Tl have no γ -emission. In the case of the cumulative production of ^{201g}Bi and ^{200}Tl the parent nucleus or the internally decaying isomeric state has a half-life similar to that of the daughter state and separate assessment is not possible. Some of the produced radio-nuclei have half-lives that are too short compared to the experimental circumstances (long waiting time in high energy irradiation) resulting in activities at the moment of first measurement below the detection limits of our spectrometric set-up.

3.2.1 Bismuth isotopes

The investigated radioisotopes of bismuth are produced only directly via $^{nat}\text{Pb}(d,xn)$ reactions.

Production of ^{207}Bi

The reaction cross-sections of ^{207}Bi ($T_{1/2} = 31.55$ a) are shown in Fig 2, together with the earlier experimental results and theoretical estimations. The new experimental data are higher compared to Ditroi et al. [3] and are in good agreement with the results of Wasilyevski et al. [4]. By comparing with theoretical results disagreements in the maximum and in the high energy pre-compound tail can be seen. The earlier versions of

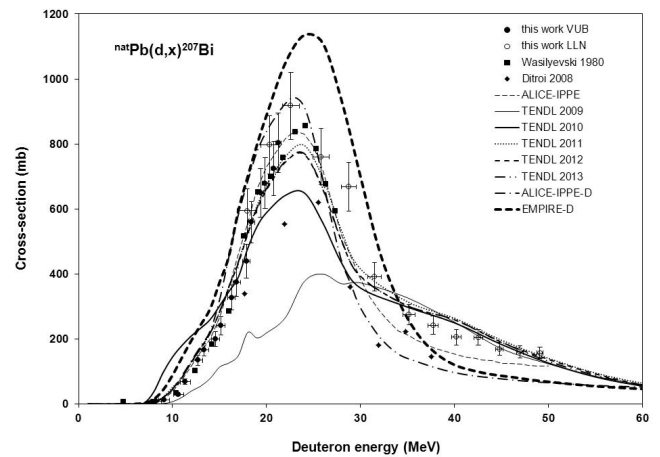


Fig. 2 Excitation function of the $^{nat}\text{Pb}(d,x)^{207}\text{Bi}$ reaction compared with the theory and literature

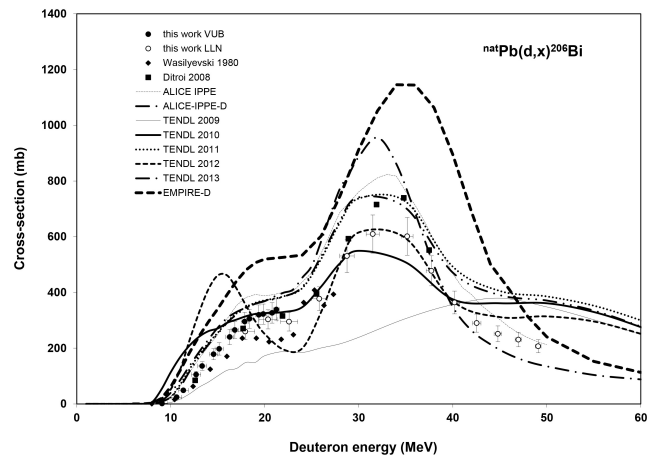


Fig. 3 Excitation function of the $^{nat}\text{Pb}(d,x)^{206}\text{Bi}$ reaction compared with the theory and literature

the TENDL libraries (From 2010 back) differ significantly from the experimental data. TENDL-2012 and 2013 seems to be identical. EMPIRE-D strongly overestimates the experimental data, while ALICE-IPPE seems to be better than the modified ALICE-IPPE-D.

Production of ^{206}Bi

The agreement between the different sets of experimental production cross-section data for ^{206}Pb ($T_{1/2} = 6.243$ d) is acceptable, except the energy region around 20 MeV (see Fig. 3). The theoretical results show large disagreement both in shape and in the magnitude. Especially TENDL-2012 shows large discrepancies compared to both TENDL-2011 and TENDL-2013. The ALICE results also overestimate the experimental values, the worst behavior is observed by EMPIRE.

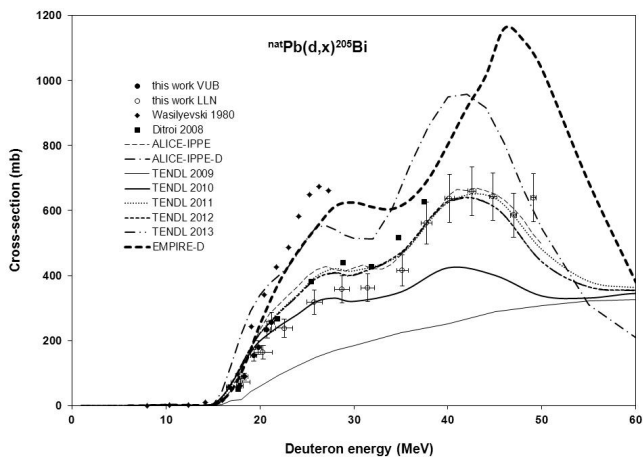


Fig. 4 Excitation function of the $^{nat}\text{Pb}(d,x)^{205}\text{Bi}$ reaction compared with the theory and literature

Production of ^{205}Bi

For ^{205}Bi ($T_{1/2} = 15.31$ d) there are large differences between the present experimental data and the results of Wasiļevski et al. [4], while a reasonable agreement is seen with Ditrói et al. [3]. The ALICE-IPPE-D and the EMPIRE-D code results overestimate the presently measured data (Fig. 4). The improvement of the different versions of the TENDL libraries is well demonstrated in this figure.

Production of ^{204}Bi

The experimental data for production of ^{204}Bi ($T_{1/2} = 11.22$ h) according to Fig. 5 show good agreement with the theoretical data in the latest TENDL libraries and the older ALICE-IPPE calculations. In this case the newest TENDL-2013 seems to be worse than the previous two above 40 MeV. The predictions of the ALICE-D and the EMPIRE-D are systematically high, especially in the energy region above 25 MeV.

Production of ^{203}Bi

The different sets of experimental activation cross-sections of the ^{203}Bi ($T_{1/2} = 11.76$ h) show good agreement with the latest three TENDL data (Fig. 6). The predictions of the ALICE-D and the EMPIRE-D are systematically high.

Production of ^{202}Bi

No earlier experimental data were found. The agreement of our experimental data with the theoretical predictions for production of ^{202}Bi ($T_{1/2} = 1.71$ h) is the best in case of TENDL-2012 (see Fig. 7).

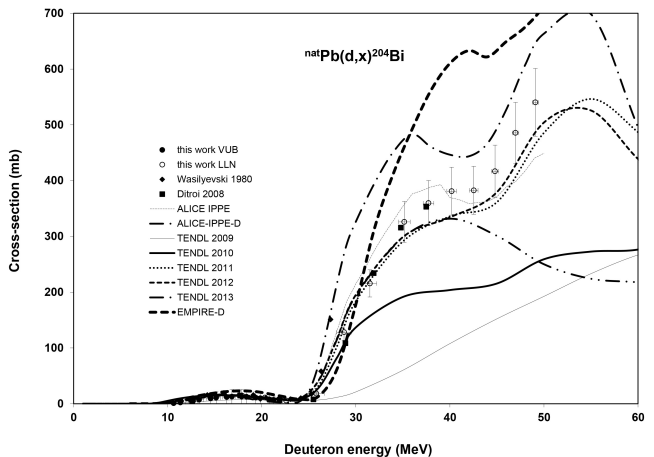


Fig. 5 Excitation function of the $^{nat}\text{Pb}(d,x)^{204}\text{Bi}$ reaction compared with the theory and literature

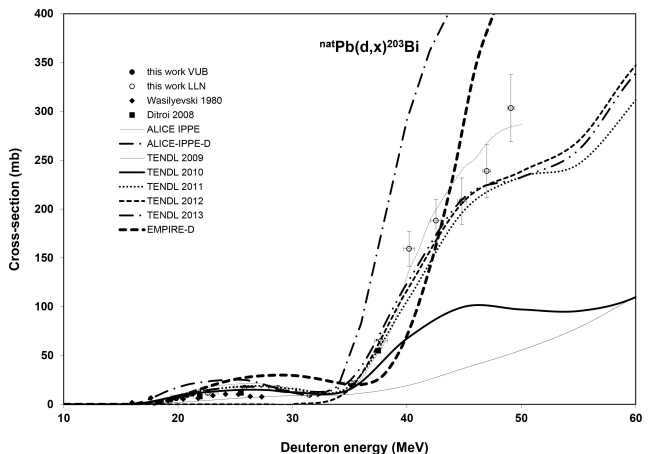


Fig. 6 Excitation function of the $^{nat}\text{Pb}(d,x)^{203}\text{Bi}$ reaction compared with the theory and literature

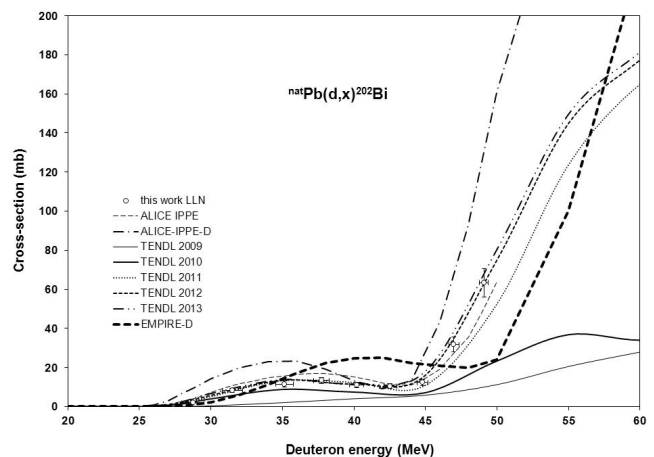


Fig. 7 Excitation function of the $^{nat}\text{Pb}(d,x)^{202}\text{Bi}$ reaction compared with the theory

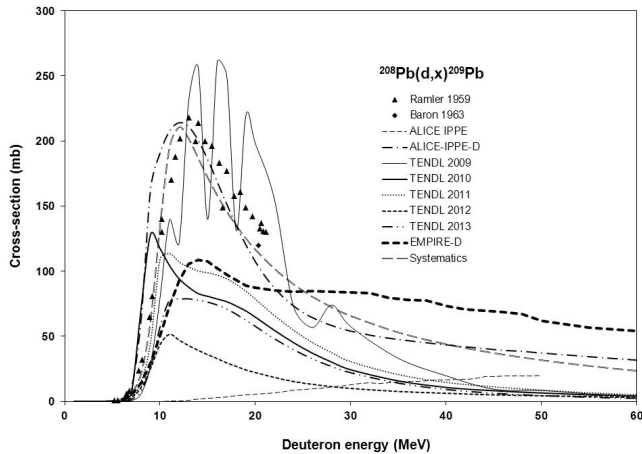


Fig. 8 Excitation function of the $^{nat}\text{Pb}(d,x)^{209}\text{Pb}$ reaction calculated by the theory and literature data

3.2.2 Lead isotopes

The investigated radioisotopes of lead are produced directly via (d,pxn) reactions and through EC, β^+ decay of the parent bismuth radioisotopes.

Production of ^{209}Pb

As it was mentioned earlier ^{209}Pb produced via the $^{208}\text{Pb}(d,p)$ reaction ($T_{1/2} = 3.253$ h, β^- : 100 %) was not detected in this experiment due to lack of γ -lines. In several of our earlier investigations we obtained experimental results for (d,p) reactions that were used to develop and implement improvements for the description of the (d,p) process in the model codes. Therefore in this work we made new theoretical calculation for this reaction using the upgraded ALICE-IPPE-D and EMPIRE-D codes and compared these results with the experimental data available in the literature (γ -measurements), with the excitation function based on experimental data of the (d,p) reaction in this mass region (systematics) and with results of the TALYS code in the TENDL libraries. As it is shown in Fig. 8, there is acceptable good agreement of the literature experimental data for ^{209}Pb production with the systematics and with ALICE-IPPE-D results. The EMPIRE-D and TENDL data significantly underestimate the maximum.

Production of ^{203g}Pb

The radioisotope ^{203g}Pb ($T_{1/2} = 51.92$ h) is produced directly, through the internal decay of the short half-life isomeric state (6.21 s) and from the decay of the ^{203}Bi ($T_{1/2} = 11.76$ h) parent. In Fig. 9 we present experimental data for the cumulative production, mea-

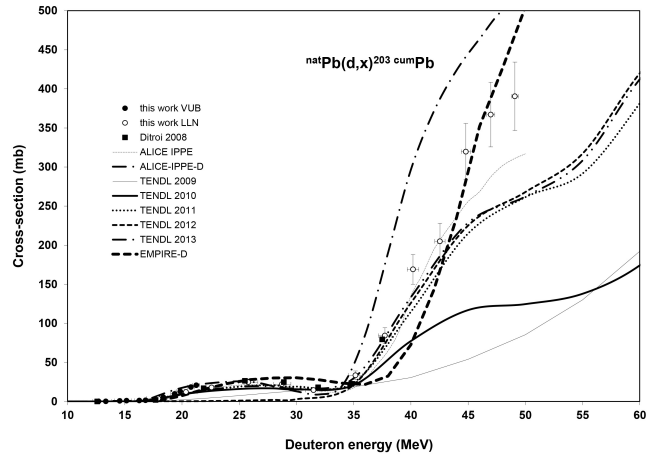


Fig. 9 Excitation function of the $^{nat}\text{Pb}(d,x)^{203g}\text{Pb}$ (cum) reaction compared with the theory and literature

sured after complete decay of all states contributing indirectly, in comparison with the earlier result of Ditroi et al. [3] and with the results of the theoretical calculations. Best agreement was found in this case with the EMPIRE-D results. The last three versions of TENDL run almost together.

Production of ^{202m}Pb

Out of the two isomeric states of ^{202}Pb the ground state has a very long half-life ($5.25 \cdot 10^4$ a) and the decay is not followed by γ -emission. We could measure the activation cross-sections only for production of the shorter-lived (3.54 h) isomeric state. This state is produced only directly, as ^{202}Bi ($T_{1/2} = 1.71$ h) decays only to the ground state of ^{202}Pb . No earlier experimental data were found in the literature. The experimental and the theoretical excitation functions are shown in Fig. 10. The theoretical results show large disagreement in the investigated energy range.

Production of ^{201}Pb

The activation cross-sections for cumulative production of ^{201}Pb ground state ($T_{1/2} = 9.33$ h) were measured after the decay of metastable ^{201m}Pb ($T_{1/2} = 61$ s) and of both isomeric states of the parent ^{201}Bi ($T_{1/2} = 59.1$ min and 103 min respectively). The experimental and theoretical data are shown in Fig. 11. There is no significant difference between the last 3 TENDL versions up to 50 MeV and those give the best approximation with a little overestimation above 45 MeV.

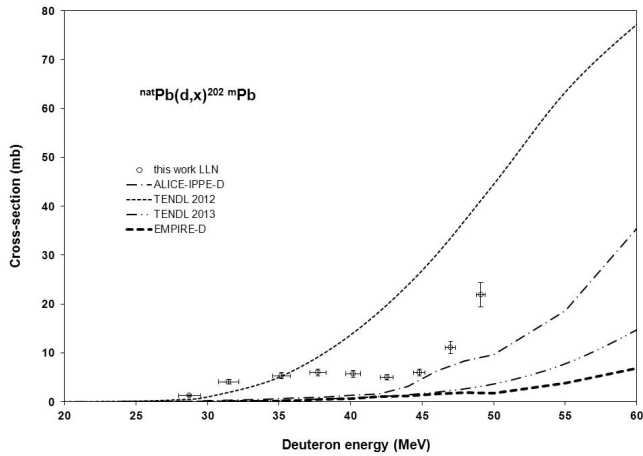


Fig. 10 Excitation function of the $^{nat}\text{Pb}(d,x)^{202m}\text{Pb}$ reaction compared with the theory and literature

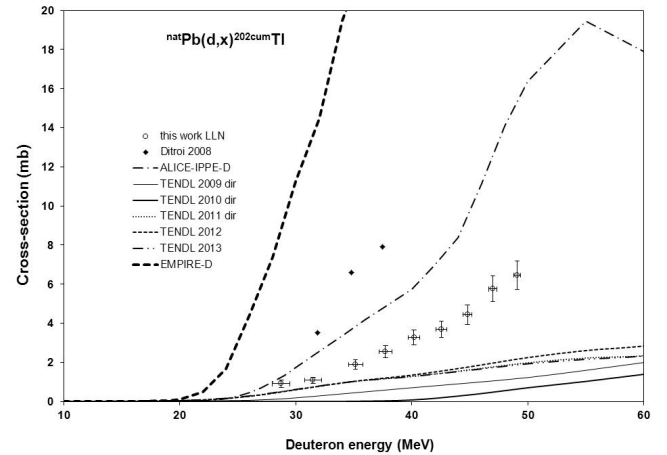


Fig. 12 Excitation function of the $^{nat}\text{Pb}(d,x)^{202}\text{Tl}(\text{cum})$ reaction compared with the theory and literature

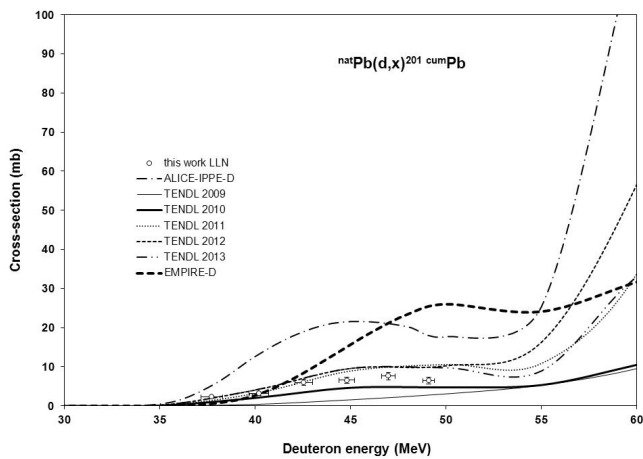


Fig. 11 Excitation function of the $^{nat}\text{Pb}(d,x)^{201}\text{Pb}(\text{cum})$ reaction compared with the theory and literature

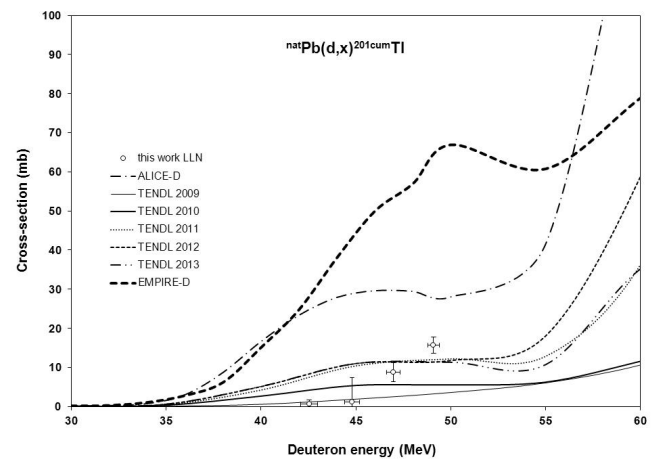


Fig. 13 Excitation function of the $^{nat}\text{Pb}(d,x)^{201}\text{Tl}(\text{cum})$ reaction compared with the theory and literature

3.2.3 Thallium isotopes

The measured radioisotopes of thallium are produced directly via $(d,2pxn)$ reactions and through EC decay of parent Pb radioisotopes.

Production of ^{202}Tl

The cumulative activation cross-sections of ^{202}Tl ($T_{1/2} = 12.31$ d) contain the direct production and the decay of ^{202m}Pb ($T_{1/2} = 3.54$ h). The contribution from the decay of ^{202g}Pb is negligible due to its very long half-life ($T_{1/2} = 5.25 \cdot 10^4$ a). The new data are lower compared to our earlier results (Ditróí et al. [3]) (Fig. 12). No theoretical results for the ^{202m}Pb in the earlier TENDL libraries, therefore only the TENDL-2012 and TENDL-2013 data are shown. None of the codes describes reasonably the cumulative production.

Production of ^{201}Tl

The measured production cross-sections of ^{201}Tl ($T_{1/2} = 3.0421$ d) are cumulative and include the decay chain contributions of the shorter-lived parent ^{201}Bi ($T_{1/2} = 5.91$ min and 1.8 h), and ^{201}Pb ($T_{1/2} = 9.33$ h and 61 s) radioisotopes. The measured cross-sections are shown in Fig. 13. No earlier experimental data were found. Because of the only few measured points it is difficult to judge between the theoretical model calculation curves.

3.3 Production yields

By fitting and integrating the measured excitation functions we have deduced integral yields for the investigated reactions (Fig. 14-15). The calculated values of $^{207,206,205}\text{Bi}$ were compared with the experimental thick

Table 2 Measured cross-sections of the bismuth isotopes in LNL and VUB laboratories

Lab.	Energy E+ Δ E(MeV)		²⁰⁷ Bi		²⁰⁶ Bi		²⁰⁵ Bi		²⁰⁴ Bi		²⁰³ Bi		²⁰² Bi		
			$\sigma \pm \Delta\sigma$ (mb)	$\sigma \pm \Delta\sigma$ (mb)	$\sigma \pm \Delta\sigma$ (mb)	$\sigma \pm \Delta\sigma$ (mb)	$\sigma \pm \Delta\sigma$ (mb)	$\sigma \pm \Delta\sigma$ (mb)	$\sigma \pm \Delta\sigma$ (mb)	$\sigma \pm \Delta\sigma$ (mb)	$\sigma \pm \Delta\sigma$ (mb)	$\sigma \pm \Delta\sigma$ (mb)	$\sigma \pm \Delta\sigma$ (mb)	$\sigma \pm \Delta\sigma$ (mb)	
LNL	17.9	1.0	594.1	67.0	259.7	29.2	72.5	9.5	14.2	1.7	1.5	0.4			
	20.4	1.0	796.1	89.6	303.4	34.2	164.5	20.6	11.1	1.3	8.2	1.3			
	22.6	0.9	916.8	103.1	295.0	33.2	238.0	28.9	5.9	0.8	11.7	1.8			
	25.8	0.8	760.5	86.3	377.4	42.4	318.9	37.4	18.3	2.1	17.0	2.2			
	28.7	0.8	668.3	75.3	531.0	59.7	358.4	41.6	128.3	14.5	16.7	2.3	2.0	0.4	
	31.5	0.7	390.6	44.0	609.6	68.5	362.5	42.0	215.6	24.3	9.6	1.8	8.3	1.0	
	35.2	0.6	274.0	31.0	601.6	67.6	415.8	48.1	326.0	36.7	21.5	3.2	11.5	1.5	
	37.7	0.6	241.5	28.2	477.6	53.7	561.3	64.3	359.6	40.4	64.9	7.4	13.3	1.6	
	40.2	0.5	205.4	23.7	364.0	41.0	637.2	73.2	381.1	42.9	159.2	18.2	11.1	1.5	
	42.5	0.5	204.1	23.9	290.0	32.6	659.8	75.3	382.6	43.0	188.2	21.5	10.5	1.3	
	44.8	0.4	168.7	19.9	251.5	28.3	642.3	73.5	416.8	46.9	208.1	23.7	12.3	1.5	
	47.0	0.3	159.2	18.5	230.9	26.0	585.6	67.2	485.6	54.6	238.9	27.2	31.8	3.7	
	49.1	0.3	156.8	18.4	207.0	23.3	639.4	73.1	540.2	60.7	303.4	34.4	63.4	7.2	
	VUB	8.2	0.6	7.5	1.6										
		9.1	0.6	12.7	2.1	1.4	0.2								
		10.6	0.5	29.0	4.5	24.2	2.7			0.9	0.1				
11.4		0.5	67.7	8.4	48.9	5.5			2.1	0.2					
12.7		0.5	134.2	15.7	105.4	11.8			5.0	0.6					
13.3		0.5	166.3	19.1	136.1	15.3			7.1	0.8					
14.6		0.5	200.0	23.1	178.5	20.1			9.4	1.1					
15.2		0.4	240.8	28.3	197.4	22.2			10.7	1.2					
16.3		0.4	327.3	38.3	240.2	27.0			11.7	1.3					
16.8		0.4	373.9	43.8	265.2	29.8	56.9	7.0	12.7	1.4					
17.9		0.4	438.7	51.7	295.4	33.2	60.8	7.4	12.7	1.4					
18.4		0.4	558.8	64.1	305.5	34.3	89.0	10.5	12.4	1.4	2.2	0.3			
19.4		0.3	648.9	75.0	319.5	35.9	153.8	17.7	10.7	1.2	4.9	0.6			
19.9		0.3	679.4	78.1	322.4	36.2	179.1	20.5	9.7	1.1	6.1	0.7			
20.8		0.3	724.6	83.2	326.8	36.7	233.4	26.5	7.8	0.9	9.3	1.1			
21.2		0.3	803.0	92.2	338.6	38.0	256.7	29.1	6.9	0.8	10.8	1.2			

Table 3 Measured cross-sections of the bismuth isotopes in LNL and VUB laboratories

Lab.	Energy E+ Δ E(MeV)		²⁰³ Pb		^{202m} Pb		²⁰¹ Pb		²⁰² Tl		²⁰¹ Tl $\sigma \pm \Delta\sigma$ (mb)		
			$\sigma \pm \Delta\sigma$ (mb)	$\sigma \pm \Delta\sigma$ (mb)	$\sigma \pm \Delta\sigma$ (mb)	$\sigma \pm \Delta\sigma$ (mb)	$\sigma \pm \Delta\sigma$ (mb)	$\sigma \pm \Delta\sigma$ (mb)	$\sigma \pm \Delta\sigma$ (mb)	$\sigma \pm \Delta\sigma$ (mb)	$\sigma \pm \Delta\sigma$ (mb)		
LNL	17.9	1.0	3.9	0.6									
	20.4	1.0	12.1	1.4									
	22.6	0.9	17.9	2.0									
	25.8	0.8	24.8	4.1									
	28.7	0.8	22.2	2.5	1.3	0.2			0.9	0.2			
	31.5	0.7	14.6	1.7	4.1	0.5			1.1	0.2			
	35.2	0.6	33.5	5.5	5.3	0.6			1.9	0.2			
	37.7	0.6	84.2	10.1	6.0	0.7	2.3	0.3	2.5	0.3			
	40.2	0.5	169.0	19.0	5.7	0.7	3.1	0.4	3.3	0.4			
	42.5	0.5	205.0	23.0	5.0	0.6	6.0	0.7	3.7	0.4	0.6	1.0	
	44.8	0.4	319.6	36.1	5.9	0.7	6.5	0.8	4.4	0.5	1.1	6.3	
	47.0	0.3	367.1	41.3	11.0	1.3	7.6	0.9	5.8	0.7	8.8	2.5	
	49.1	0.3	390.4	43.8	21.8	2.5	6.4	0.8	6.5	0.7	15.7	2.1	
	VUB	12.7	0.5	0.09	0.21								
		13.3	0.5	0.14	0.13								
		14.6	0.5	0.79	0.15								
15.2		0.4	1.1	0.17									
16.3		0.4	1.1	0.17									
16.8		0.4	1.4	0.20									
17.9		0.4	3.4	0.42									
18.4		0.4	5.3	0.62									
19.4		0.3	9.6	1.1									
19.9		0.3	12.8	1.5									
20.8		0.3	18.4	2.1									
21.2	0.3	20.8	2.3										

target yields available in the literature (Dmitirev et al. [5]) (Fig. 14). The yields of the rest of the measured isotopes are presented in Fig. 15. No literature data were found for these isotopes. In Fig. 14 it is seen that the largest yield can be achieved by ²⁰⁶Bi the previous results of Dmitirev [5] is in good agreement with our results on ²⁰⁷Bi and somewhat higher in the case of ²⁰⁶Bi and ²⁰⁵Bi. In Fig. 15 much larger yield are also presented (e.g. ²⁰⁴Bi) and the range of yield covers even four orders of magnitude by 30 MeV.

4 Summary and conclusions

Lead is a metallic material, which is frequently used as construction material and alloy component in industry and in nuclear technology, including accelerator tech-

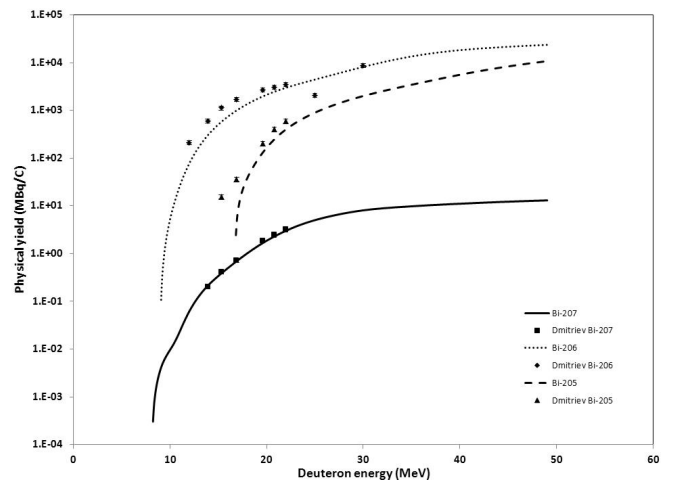


Fig. 14 Calculated integral yields of ^{205,206,207}Bi on natural lead target, compared with the literature

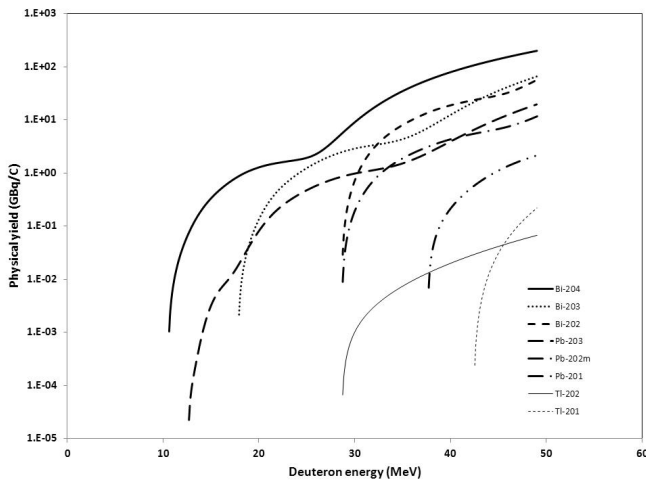


Fig. 15 15. Calculated integral yields of $^{204,203,202}\text{Bi}$, $^{203,202m,201}\text{Pb}$ and $^{202,201}\text{Tl}$ on natural lead target

nology (fusion, shielding and target technology, accelerator driven waste transmutation, etc.). Experimental cross-sections and derived integral yields are reported for the $^{nat}\text{Pb}(d,x)^{206,205,204,203,202}\text{Bi}$, $^{203cum,202m,201cum}\text{Pb}$ and $^{202cum,201cum}\text{Tl}$ reactions. The comparison with the earlier experimental data in the literature shows large disagreement in a few cases. The agreement with the theoretical predictions is also moderate for all model codes. The new versions of the TENDL library result mostly in better agreement with the experimental data. It is hard to explain the large disagreement of the earlier TENDL versions. In case of ALICE and EMPIRE systematic overestimation can be observed. Reliable experimental activation data are important for further improving the predictive power of the presently available theoretical codes. The present experimental data extend the energy range and the list reactions, for which comparison with the different model codes can be made, showing the need for better description of deuteron induced reactions in the nuclear model codes.

Acknowledgements This work was done in the frame MTA-FWO research project and collaboration. The authors acknowledge the support of research projects and of their respective institutions in providing the materials and the facilities for this work.

References

1. F. Tárkányi, A. Hermanne, F. Ditrói, S. Takács, B. Király, G. Csikai, M. Baba, H. Yamazaki, M.S. Uddin, A.V. Ignatyuk, S.M. Qaim. Systematic study of activation cross-sections of deuteron induced reactions used in accelerator applications (2011)
2. A. Hermanne, F. Tárkányi, S. Takács. Production of medically relevant radionuclides with medium energy deuterons (2008)
3. F. Ditrói, F. Tárkányi, S. Takács, M.S. Uddin, M. Hagiwara, M. Baba, A. Ignatyuk, S.F. Kovalev, Journal of Radioanalytical and Nuclear Chemistry **276**(3), 835 (2008)
4. C. Wasilevsky, M. De La Vega Vedoya, J. Nassiff S, Radiochimica Acta **27**(3), 125 (1980)
5. P.P. Dmitriev, N.N. Krasnov, G.A. Molin, M.V. Panarin, Soviet Atomic Energy **33**(4), 976 (1972)
6. F. Tárkányi, A. Hermanne, S. Takács, F. Ditrói, A.I. Dityuk, Y.N. Shubin, Nuclear Instruments & Methods in Physics Research Section B-Beam Interactions with Materials and Atoms **217**(3), 373 (2004)
7. A. Hermanne, R.A. Rebeles, F. Tárkányi, S. Takács, M.P. Takács, J. Csikai, A. Ignatyuk, Nuclear Instruments & Methods in Physics Research Section B-Beam Interactions with Materials and Atoms **270**, 106 (2012)
8. S. Takács, M.P. Takács, A. Hermanne, F. Tárkányi, R.A. Rebeles, Nuclear Instruments & Methods in Physics Research Section B-Beam Interactions with Materials and Atoms **278**, 93 (2012)
9. F. Tárkányi, F. Ditrói, A. Hermanne, S. Takács, A.V. Ignatyuk, Journal of Radioanalytical and Nuclear Chemistry **298**, 277 (2013)
10. R.R. Kinsey, C.L. Dunford, J.K. Tuli, T.W. Burrows. Nudat 2.6 <http://www.nndc.bnl.gov/nudat2/> (1997)
11. H.H. Andersen, J.F. Ziegler, *Hydrogen stopping powers and ranges in all elements. The stopping and ranges of ions in matter, Volume 3.* The Stopping and ranges of ions in matter (Pergamon Press, New York, 1977)
12. F. Tárkányi, S. Takács, K. Gul, A. Hermanne, M.G. Mustafa, M. Nortier, P. Oblozinsky, S.M. Qaim, B. Scholten, Y.N. Shubin, Z. Youxiang. Charged particles cross-sections database for medical radioisotope production, beam monitors reactions (2001)
13. A.I. Dityuk, A.Y. Konobeyev, V.P. Lunev, Y.N. Shubin, New version of the advanced computer code alice-ippe. Tech. rep., IAEA (1998)
14. M. Herman, R. Capote, B.V. Carlson, P. Oblozinsky, M. Sin, A. Trkov, H. Wienke, V. Zerkin, Nuclear Data Sheets **108**(12), 2655 (2007)
15. F. Tárkányi, A. Hermanne, S. Takács, K. Hilgers, S.F. Kovalev, A.V. Ignatyuk, S.M. Qaim, Applied Radiation and Isotopes **65**(11), 1215 (2007)
16. A. Hermanne, F. Tárkányi, S. Takács, F. Ditrói, M. Baba, T. Ohtshuki, I. Spahn, A.V. Ignatyuk, Nuclear Instruments & Methods in Physics Research Section B-Beam Interactions with Materials and Atoms **267**(5), 727 (2009)
17. A.V. Ignatyuk. Phenomenological systematics of the (d,p) cross sections, [http://www-nds.iaea.org/fendl3/000pages/rcm3/slides//ignatyuk_fendl-3\(2011\)](http://www-nds.iaea.org/fendl3/000pages/rcm3/slides//ignatyuk_fendl-3(2011))
18. A.J. Koning, D. Rochman, S. van der Marck, J. Kopecky, J.C. Sublet, S. Pomp, H. Sjostrand, R. Forrest, E. Bauge, H. Henriksson, O. Cabellos, S. Goriely, J. Leppanen, H. Leeb, A. Plompen, R. Mills. Tendl-2013: Talys-based evaluated nuclear data library (2012)
19. A.J. Koning, D. Rochman, Nuclear Data Sheets **113**, 2841 (2012)